EXPERIMENTAL STUDY OF DIFFUSER CHANNELS WITH A NEAR-SEPARATING TURBULENT BOUNDARY LAYER

L. A. Bychkova

UDC 532.556.4

Results of experimental studies are shown concerning the aerodynamic characteristics of diffusers with the transition profile designed for a near-separating turbulent boundary layer. The test results are shown to agree closely with calculations.

The choice of optimal transition profiles in diffusers ensures a maximum deceleration of the stream within a given length of path. Experimental studies of conical diffusers have shown that, within the region of adhesive flow, the losses in total pressure decrease as the divergence angle increases, until separation occurs at some section [1]. Thus, the pressure is recovered best in a near-separation mode of flow, while the losses will sharply increase once separation occurs.

It is reasonable to suppose that one possible method of reducing the losses during deceleration of a stream would be to profile the diffuser wall in such a way as to make the flow at every channel section sufficiently close to separation (surface friction $\tau_W \equiv 0$). A channel with a transition profile based on this consideration should have the optimal aerodynamic characteristics. The idea was disclosed in the nineteen thirties by Dointsyanskii [2]. The profile of a diffuser with a circular or flat cross section and with a near-separation boundary layer, i.e., a so-called "near-separation" diffuser has the shape of a bell. At the entrance section of such a channel, where the boundary layer is relatively thin, the local divergence angles may be large but, as the boundary layer becomes thicker, they should decrease so as to impart to the flow its maximum capability of overcoming local pressure gradients without separation along the entire channel.

Near-separation turbulent flow at a flat wall was realized in [3, 4]; it has been revealed that such a flow is rather stable. Bell-shaped diffusers the profile of which almost satisfies the conditions for a near-separation boundary layer, as explained in [5, 6], are often more efficient than diffusers with straight walls and adhesive flow. The advantage here may be either in terms of reduced losses per certain channel length or in terms of reduced axial dimensions at the same efficiency level.

An approximate method of calculating the geometry and the aerodynamic characteristics of near-separation diffusers with a flat or circular cross section has been outlined in [2]. This method is based on known relations for a two-dimensional and an axially symmetrical turbulent boundary layer at separation [7]. Naturally, using the simplest approximate method for calculating the turbulent boundary layer will yield a certain approximation in the final results. At the same time, however, it can reveal the basic character of the relations which govern the performance of diffusers with near-separation flow. Applying more complex theories, on the other hand, would hardly be justified. This is because, first of all, such theories become unwieldy even for a two-dimensional boundary layer and such theories fully accounting for the effects of transverse surface curvature have not yet been developed for an axially symmetrical boundary layer.

The theoretical study of near-separation diffusers in [2] was based on the following assumptions: that the flow is incompressible, that the static pressure across the channel is invariable, and that the turbulent boundary layer is about to separate along the entire channel ($\tau_W = 0$). In this article we will use the formulas which have been derived in [2] for determining the characteristics of the entrance stage (in the presence of a potential-flow nucleus) of circular diffusers:

Translated from Inzhenerno-Fizicheskii Zhurnal, Vol. 21, No. 3, pp. 518-523, September, 1971. Original article submitted November 10, 1970.

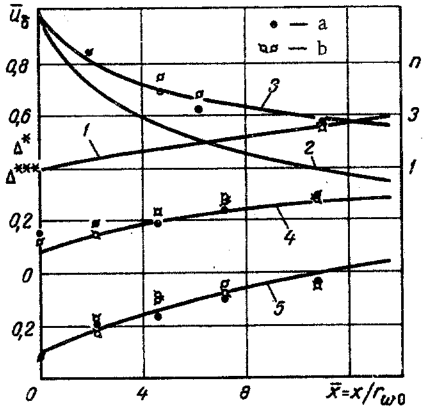

Fig. 1

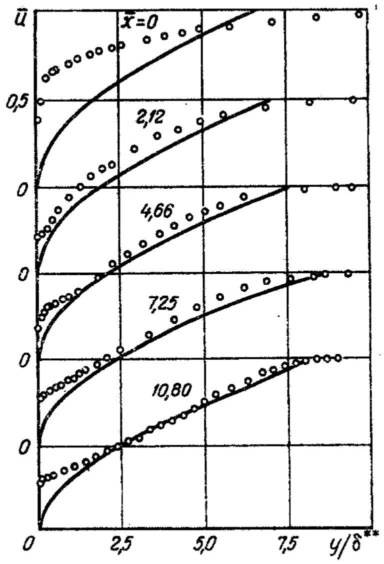

Fig. 2

Fig. 1. Comparison of theoretical and experimental values for a circular diffuser profiled according to the criteria $\Delta_0^* = 0.1$, k = 0.325, $\tau_W = 0$: 1) n; 2) $\bar{u}_{\delta i}$; 3) $\bar{u}_\delta$, $u_{\delta i}$; 4) Δ^{***}; 5) Δ^*.

Fig. 2. Distortion of velocity profiles in the diffuser ($\Delta_0^* = 0.1$, k = 0.325).

divergence index

$$n = \frac{1}{\bar{u}_\delta}\left\{1 - \Delta_0^*\left[1 - \frac{H}{H_0}\bar{u}_\delta^{-[1+0.5(H+H_0)]}\right]\right\};$$

velocity outside the boundary layer

$$\bar{u}_\delta = u_\delta/u_{\delta 0} = \Phi^\beta,$$

$$\beta = [1 + 0.5(H + H_0)]^{-1},\quad \Phi = \frac{1}{1-\Delta_0^*}\cdot\frac{2\bar{\delta}_0 - \bar{\delta}_0^2}{2\bar{\delta} - \bar{\delta}^2}\cdot\frac{H_0^{**}}{H^{**}} - \frac{H}{H_0}\Delta_0^*;$$

coefficient of total-pressure loss

$$\zeta = \frac{\Delta^{***}}{n^2(1-\Delta^*)^3} - \frac{\Delta_0^{***}}{(1-\Delta_0^*)^3};$$

and variation along the axial coordinate ξ

$$\xi = k^2 x/r_{w0} = -4\int_1^{\bar{u}_\delta}\frac{\bar{\delta}\sqrt{n}}{\bar{u}_\delta P^2},\quad P = \sqrt{\bar{\delta}}/E(\varphi_\delta;\ \theta).$$

Here k is an empirical constant in the expression for the displacement path $l = ky$; $E(\varphi_\delta;\ \theta)$ is an elliptic integral of the second kind with the argument $\varphi_\delta = \sin^{-1}\sqrt{\bar{\delta}}$ and with the modulus $\cos\theta = \sqrt{2}/2$; $\Delta = \vartheta/F$; $\Delta^* = \vartheta^*/F$; $\Delta^{**} = \vartheta^{**}/F$; $\Delta^{***} = \vartheta^{***}/F$; $H = \Delta^*/\Delta^{**}$; $H^{**} = \Delta^{**}/\Delta$; and $\bar{\delta} = \delta/r_W$.

The calculation method is an approximate one, since it is based on the simplest approximation for the friction distribution and for the mixing length across the boundary layer. The design-theoretical analysis becomes much simpler if a near-separating turbulent boundary layer is assumed along the entire channel – even at the entrance section. In reality, though, if separation does not begin at the entrance, near-separation flow can exist only at some distance behind the entrance. In the latter case there will be a segment along which transition from adhesive to near-separation flow takes place. The existence of such a transitional channel segment may cause the aerodynamic characteristics of the channel to depend on the Reynolds number at the entrance. For a complete near-separation flow, in the meantime, the Reynolds number has no effect on the boundary layer and thus on the diffuser characteristics.

According to the formulas given here, the geometry and the aerodynamic characteristics of near-separation diffusers depend on the single parameter Δ_0^*, which represents the effect of initial flow

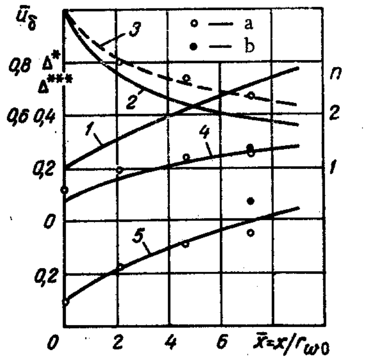

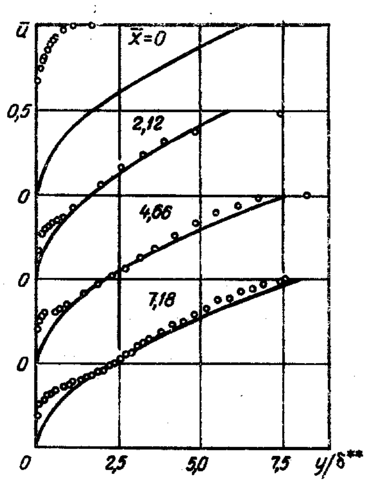

Fig. 3   Fig. 4

Fig. 3. Comparison of theoretical and experimental values for a circular diffuser profiled to conform to $\Delta_0^* = 0.1$, k = 0.400, $\tau_w = 0$: 1) n; 2) $\bar{u}_\delta$; 3) $\bar{u}_{\delta 1}$; 4) Δ^{***}; 5) Δ^*.

Fig. 4. Distortion of velocity profiles in the diffuser ($\Delta_0^* = 0.1$, k = 0.400).

nonuniformity at the entrance. Indeed, it follows from the continuity equation that this parameter defines uniquely the mean-to-maximum velocity ratio at the entrance section:

$$\Delta_0^* = 1 - \frac{u_0}{u_{\delta 0}}.$$

The derived equations are valid for $\Delta_0^* > 0$ and become meaningless when $\Delta_0^* = 0$, since near-separation flow at the entrance is not possible then.

The results of calculations have shown that, as the initial nonuniformity increases, the divergence index over a given diffuser length decreases while the loss coefficient increases.

In order to design the diffuser profile, one must know the value of the empirical constant k. This constant appears as a multiplier in the expression for the axial coordinate ξ and this makes it possible qualitatively to determine the basic trends of near-separation diffuser characteristics, even if the value of the empirical constant is unknown.

The value of k was first roughly determined from a very limited amount of available data on near-separation flow at a channel wall, whereupon it was refined during the experiment. Changing the value of k caused only a uniform distortion of the ξ-coordinate. A comparison of our calculations with the data obtained by Stratford [3] and Nestler [8] gave k = 0.325–0.400. By assigning the smaller value to k in our calculations, we have elongated the diffuser and eliminated the hazard of possible separation, but then a near-separation flow may also not have been realizable. The problem in the study of near-separation diffusers with a circular cross section is that the geometry of a model cannot be adjusted during the experiment. This makes it difficult to correct the errors of calculation and to approach near-separation flow as desired. Therefore, for a given initial flow nonuniformity, in profiling the model we first chose the smaller value for k at which the theory agreed with existing test data. The model was then bored out so as to make its profile correspond to the larger calculated value of k, which allowed us to establish the value of this empirical constant corresponding to maximum deceleration of the flow within a given channel length.

In calculating channels with a thin boundary layer at the entrance, the theoretical values of local divergence angles $\alpha/2 = 0.5 \tan^{-1} (\Pi^{-1} dF/dx)$ become excessively large ($\alpha/2 > 10°$). In such cases, in order to reduce the adverse effect of the corner point (which is disregarded in the boundary layer theory), one usually smooths out ($\alpha/2 \leq 9°$) the junction between the entrance nozzle and the diffuser. This is equivalent to reducing the peaks in the local divergence angle variation in the entrance stage and it results in a departure from the calculated model geometry. For this reason, we will consider here test data pertaining to a diffuser with a thick boundary layer at the entrance, the geometry of which conforms stringently to calculations (with $\alpha/2$ angles not exceeding 9°).

A circular diffuser with an entrance radius $r_{W0} = 42.5$ mm was designed for $\Delta_0^* = 0.1$ at $k = 0.325$. A theoretical initial nonuniformity in the velocity profile was built in by a constant-section entrance nozzle the length of which had been determined from the data in [9]. A collector was placed before the nozzle.

For testing the diffuser we used the conventional procedure of pneumometric measurements. The velocity corresponding to the initial flow nonuniformity was determined more precisely during the experiment and its constancy was checked by the pressure drop across the collector at the entrance. The static pressure was measured through drain holes in the wall which had been drilled perpendicularly to the inner surface of the channel. The velocity profiles in the boundary layer $\bar{u} = \bar{u}(y/\delta)$ were examined at several sections by means of a full-pressure micronozzle installed in a microcoordinates plotter and, on the basis of these profiles, we determined the nominal displacement areas and energy losses. The smallest step of the microcoordinates plotter was 0.02 mm. The continuity condition at the various channel sections was satisfied within an accuracy of $\pm 1\%$ during measurements.

The results of measurements and the calculated relations are shown in Fig. 1. The test data are compared here with the velocity profile corresponding to an ideal fluid flow in the channel $\bar{u}_{\delta i}$ (ideal case), with the distribution of velocities $\bar{u}_8$ (theoretical case) corresponding to a viscous fluid flow at a given initial nonuniformity of the velocity profile, and also with the calculated values of Δ^* and Δ^{***}. The variants in Fig. 1a and Fig. 1b correspond to $Re_0 = r_{W0}u_0/\nu = 0.85 \cdot 10^5$ and $1.1 \cdot 10^5$ respectively with a turbulent boundary layer at the entrance. According to the graphs, our experimental study has confirmed the validity of the basic calculated relations. The small variation in the Re_0 number had no effect on the aerodynamic characteristics. The satisfactory agreement between the theoretical and the experimental values of Δ^* and Δ^{***} allows us to conclude that the calculated coefficient of total-pressure loss ζ is sufficiently close to its test value [2].

The distortion of velocity profiles in the boundary layer is shown in Fig. 2, where a gradual transition from adhesive to near-separation flow at the entrance can be observed. The deviation of test points from those calculated near the wall is apparently caused by measurement errors due, in particular, to an eccentricity between the geometric and the effective opening in the micronozzle.

The subsequent boring of the model to conform to $k = 0.400$ did not improve the tested channel characteristics (Fig. 3). The flow in the bored-out diffuser was accompanied by considerable pressure pulsations. As is shown in Fig. 3, a velocity variation along the channel axis is not revealed so well in theory: the test curve of velocity distribution $\bar{u}_{\delta 1}(\bar{x})$ deviates noticeably from the calculated $\bar{u}_{\delta}(\bar{x})$ curve. The approach to separation is manifested by a distortion of the axial flow symmetry in the diffuser exit stage. When the displacement area at sections here was measured along one radius (variant Fig. 1a), therefore, the continuity condition was violated. At $\bar{x} = x/r_{W0} = 7.2$ the velocity profiles were measured along two mutually perpendicular diameters (variant Fig. 1b). The continuity condition was then maintained within 1%. Velocity profiles in the bored-out diffuser are shown in Fig. 4.

On the basis of this presentation, we conclude that diffusers may be designed according to the formulas in [2] with the value for the empirical constant taken as $k = 0.325$.

The author thanks A. S. Ginevskii for assistance in carrying out this work.

NOTATION

x, y	are the longitudinal and transverse coordinates;
r_W, Π, F	are the radius, circumference, and cross section area of a channel;
n	is the diffuser divergence index;
$\alpha/2$	is half of the local divergence angle;
δ, ϑ	are the thickness and area of the boundary layer;
$\vartheta^*, \vartheta^{**}, \vartheta^{***}$	are the displacement area, momentum, and energy losses;
u_0	is the velocity at the channel entrance, averaged with respect to the flow rate;
$\bar{u}_{\delta i}, \bar{u}_{\delta}, \bar{u}_{\delta 1}$	are the dimensionless velocities along the channel axis (ideal flow, calculated, and tested);
Re_0	is the Reynolds number;
ζ	is the coefficient of total-pressure loss;
k	is an empirical constant;
τ_W	is the frictional stress at the channel wall.

Subscript

0 refers to the entrance section.

LITERATURE CITED

1. I. E. Idel'chik, Hydraulic Resistances [in Russian], Gosizdat, Moscow–Leningrad (1954).
2. A. S. Ginevskii and L. A. Bychkova, in: Heat and Mass Transfer [in Russian], Vol. 1, Énergiya, Moscow–Leningrad (1968).
3. B. S. Stratford, J. Fluid Mech., 5, No. 1, 17 (1959).
4. W. G. Spangenberg, W. R. Rowland, and N. E. Mease, Fluid Mechanics of Internal Flow, General Motors Research Laboratories, Elsevier Publ. Co., Amsterdam–London–New York (1967).
5. M. Hackeschmidt, Maschinenbautechnik, 13, No. 10 (1964).
6. M. Hackeschmidt and E. Vogelsang, Wissensch. Zeitschr. der Tech. Univ. Dresden, 15, No. 1 (1966).
7. A. S. Ginevskii and E. E. Solodkin, Prikl. Matem. Mekhan., 22, No. 6, 819-825 (1958).
8. W. Nestler, Maschinenbautechnik, 19, No. 2 (1970).
9. A. S. Ginevskii, in: Industrial Aerodynamics [in Russian], No. 7, Oborongiz (1956).